NUMERICAL MODELING OF OPTICAL PARAMETRIC FREQUENCY CONVERSION

ANDERS C. BILFELDT

ERRATA

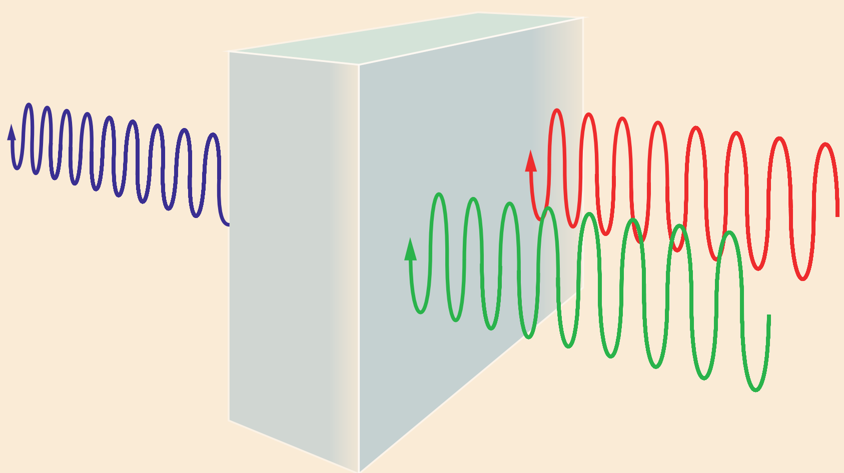

for temporally confined pulses and spatially confined modes

August 2014

3.1 MATERIAL RESPONSE, TIME-DOMAIN

$$\tilde{P}_{\mu}^{(2)}(\mathbf{r},t) = \epsilon_0 \int\limits_{-\infty}^{\infty}\int\limits_{-\infty}^{\infty} R^{(2)}_{\mu\alpha_1\alpha_2}(t-\tau_1, t-\tau_2)\tilde{E}_{\alpha_1}(\mathbf{r},\tau_1) \tilde{E}_{\alpha_2}(\mathbf{r},\tau_n)\, d\tau_1\, d\tau_2 \tag{20}$$

[Missing tilde.]

$$\tilde{P}_{\mu}^{(n)}(\mathbf{r},t) = \epsilon_0 \int_{-\infty}^{\infty} \cdots \int_{-\infty}^{\infty} R^{(n)}_{\mu\alpha_1\cdots\alpha_n}(t-\tau_1, \cdots, t-\tau_n) \tilde{E}_{\alpha_1}(\mathbf{r},\tau_1)\cdots\tilde{E}_{\alpha_n}(\mathbf{r},\tau_n)\, d\tau_1 \cdots d\tau_n \tag{21}$$

[Missing tilde.]

3.2 MATERIAL RESPONSE, FREQUENCY-DOMAIN

$$\begin{aligned}\tilde{P}_{\mu}^{(2)}(\mathbf{r},t) &= \epsilon_0 \sum_{\substack{\alpha_1,\alpha_2\\ \in(x,y,z)}} \int\limits_{-\infty}^{\infty}\int\limits_{-\infty}^{\infty} R^{(2)}_{\mu\alpha_1,\alpha_2}(\tau_1,\tau_2)\Bigg[\int\limits_{-\infty}^{\infty}\int\limits_{-\infty}^{\infty} E_{\alpha_1}(\mathbf{r},\omega_1)E_{\alpha_2}(\mathbf{r},\omega_2)e^{i(\omega_1\tau_1+\omega_2\tau_2)}e^{-i(\omega_1+\omega_2)t}\\ &\qquad d\omega_1\, d\omega_2]\, d\tau_1\, d\tau_2\\ &= \epsilon_0 \sum_{\substack{\alpha_1\alpha_2\\ \in(x,y,z)}} \int\limits_{-\infty}^{\infty}\int\limits_{-\infty}^{\infty} \chi^{(2)}_{\mu\alpha_1\alpha_2}(\omega_\sigma;\omega_1,\omega_2) E_{\alpha_1}(\mathbf{r},\omega_1)E_{\alpha_2}(\mathbf{r},\omega_2)e^{-i\omega_\sigma t}\, d\omega_1\, d\omega_2\end{aligned} \tag{25}$$

[Missing minus sign in exponential expression.]

$$\begin{aligned}\tilde{P}_{\mu}^{(n)}(\mathbf{r},t) &= \epsilon_0 \sum_{\substack{\alpha_1,\cdots,\alpha_n\\ \in(x,y,z)}} \int\limits_{-\infty}^{\infty}\cdots\int\limits_{-\infty}^{\infty} R^{(n)}_{\mu\alpha_1,\cdots,\alpha_n}(\tau_1,\ldots,\tau_n)\\ &\left[\int_{-\infty}^{\infty}\cdots\int_{-\infty}^{\infty} E_{\alpha_1}(\mathbf{r},\omega_1)\cdots E_{\alpha_n}(\mathbf{r},\omega_n)e^{i(\omega_1\tau_1+\cdots+\omega_n\tau_n)} e^{-i(\omega_1+\cdots+\omega_n)t}\, d\omega_1\cdots d\omega_n\right] d\tau_1\cdots d\tau_n\\ &= \epsilon_0 \sum_{\substack{\alpha_1,\cdots,\alpha_n\\ \in(x,y,z)}} \int_{-\infty}^{\infty}\cdots\int_{-\infty}^{\infty} \chi^{(n)}_{\mu\alpha_1\cdots\alpha_n}(\omega_\sigma;\omega_1,\ldots,\omega_n) E_{\alpha_1}(\mathbf{r},\omega_1)\cdots E_{\alpha_n}(\mathbf{r},\omega_n)e^{-i\omega_\sigma t}\, d\omega_1\cdots d\omega_n\end{aligned} \tag{26}$$

[Missing minus sign in exponential expression. Three dots instead of one dot.]

$$\mathbf{E}(\mathbf{r},\omega_j) = E(\mathbf{r},\omega_j)\hat{\mathbf{e}}^{(j)} = E(\mathbf{r},\omega_j)\sum_{\mu\in(x,y,z)} c_\mu \hat{\mathbf{e}}_\mu^{(j)} \tag{30}$$

[Missing expansion coefficients.]

$$\begin{aligned}\mathbf{P}^{(n)}(\mathbf{r},\omega) = \epsilon_0 \sum_{\mu\in(x,y,z)} \sum_{\substack{\alpha_1,\cdots,\alpha_n\\ \in(x,y,z)}} \int_{-\infty}^{\infty}\cdots\int_{-\infty}^{\infty} \\ \chi^{(n)}_{\mu\alpha_1\cdots\alpha_n}(\omega_\sigma;\omega_1,\ldots,\omega_n)E(\mathbf{r},\omega_1)c_{\alpha_1}\hat{\mathbf{e}}^{(1)}_{\alpha_1}\cdots E(\mathbf{r},\omega_n)c_{\alpha_n}\hat{\mathbf{e}}^{(n)}_{\alpha_n} \\ \delta(\omega-\omega_\sigma)\,d\omega_1\cdots d\omega_n\hat{\mathbf{e}}_\mu \\ = \epsilon_0\hat{\mathbf{e}}_p \int_{-\infty}^{\infty}\cdots\int_{-\infty}^{\infty} \chi^{(n)}_{eff}(\omega_\sigma;\omega_1,\ldots,\omega_n) \\ E(\mathbf{r},\omega_1)\cdots E(\mathbf{r},\omega_n)\delta(\omega-\omega_\sigma)\,d\omega_1\cdots d\omega_n\end{aligned} \tag{31}$$

[Missing expansion coefficients.]

$$\begin{aligned}\hat{\mathbf{e}}_p\chi^{(n)}_{eff}(\omega_\sigma;\omega_1,\ldots,\omega_n) = \\ \sum_{\substack{\mu,\alpha_1,\cdots,\alpha_n\\ \in(x,y,z)}} \chi^{(n)}_{\mu\alpha_1\cdots\alpha_n}(\omega_\sigma;\omega_1,\ldots,\omega_n)\hat{\mathbf{e}}_\mu c_{\alpha_1}\hat{\mathbf{e}}^{(1)}_{\alpha_1}\cdots c_{\alpha_n}\hat{\mathbf{e}}^{(n)}_{\alpha_n}\end{aligned} \tag{32}$$

[Missing expansion coefficients. Missing polarization unit vector.]

3.3.1 *Magnesium doped Lithium Niobate crystal*

In the simulations discussed in this project we are focusing on *magnesium doped (5%) Periodically Poled Lithium Niobate* (MgO:PPLN) crystals. The highest *effective susceptibility* for this type of crystals is for the coupling between electric fields all polarized along the extraordinary axis of the crystal, corresponding to the x-axis in laboratory coordinates according to...
[x-axis instead of y-axis]

The χ_{ccc} tensor element is utilized by polarizing all the interacting fields along the extraordinary axis, the x-axis with the choice of axis seen...
[x-axis instead of y-axis]

MgO:PPLN crystals are chosen in this thesis since it fits the requirement of DFG at pump wavelength 1064 nm, idler wavelength 1570 nm and signal wavelength 3313 nm since QPM phase match...
[3313 nm instead of 1064 nm]

4.4 SPECIAL CASES

4.4.1 *Quasi monochromatic wave*

$$\tilde{\mathbf{E}}(z,t) = \frac{1}{2}\left[\tilde{\mathbf{A}}_1(z,t)e^{i(k_{0,1}z-\omega_{0,1}t)} + \tilde{\mathbf{A}}_1^*(t,z)e^{-i(k_{0,1}z-\omega_{0,1}t)}\right] \tag{53}$$

[Missing tilde. $\tilde{\mathbf{A}}_1^*(t,z)$ instead of $\mathbf{A}, \mathbf{t}_1^*(z)$]

4.4.2 *Continuous wave*

$$\frac{\partial}{\partial t}\mathbf{A}(\mathbf{r},t) = 0 \tag{54}$$

[Missing tilde. $\mathbf{A}(\mathbf{r},t)$ instead of $\mathbf{E}(\mathbf{r},t)$]

4.4.3 *Plane wave*

$$\nabla_\perp \tilde{\mathbf{A}}(\mathbf{r},t) = 0 \tag{55}$$

[Missing tilde.]

4.4.4 *Slowly Varying Envelope Approximation*

$$\frac{\partial^2}{\partial z^2}\tilde{\mathbf{A}}(\mathbf{r},t) \ll 2ik_0\frac{\partial}{\partial z}\tilde{\mathbf{A}}(\mathbf{r},t) \tag{56}$$

[Missing tilde.]

4.5 MONOCHROMATIC SPATIAL WAVE

4.5.1 *Orthonormal basis of Laguerre-Gaussian modes*

c_{lp} is an appropriate normalization constant
[c_{lp} instead of C_{lp}^{LG}].

$$A_j(r,\theta,z) = \sum_{p\geqslant 0} C_{j,p,0}u_{j,p,0}(r,\theta,z) \tag{59}$$

[Missing expansion coefficients.]

5.1 SECOND HARMONIC

5.1.1 *Slowly varying, monochromatic, plane wave*

where it is assumed that $\chi^{(2)}_{eff} = \chi^{(2)}_{eff}(2\omega_{0,1}; \omega_{0,1}, \omega_{0,1}) = \ldots$
[$\chi^{(2)}_{eff}(2\omega_{0,1}; \omega_{0,1}, \omega_{0,1})$ instead of $\chi^{(2)}_{eff}(2\omega_{0,1}; \omega_{0,1})$].

...since all interacting fields are polarized along the extraordinary axis of the crystal, the x-axis according...
[x-axis instead of y-axis.]
Difference Frequency Generation is the process of two incoming fields, ω_2 and ω_3 generates a field of the difference frequency $\omega_1 = \omega_3 - \omega_2$. [Inconsistency with naming of signals in figure and caption.]

5.3 DEPLETION

The *weak coupling approximation* is the assumption that the pump wave only transfers a small fractions of energy to the idler and signal meaning that the amplitude is approximately constant along the crystal, $\frac{da_{\omega_3}}{dz} = 0$.
[a_{ω_3} instead of a_{ω_1}.]

5.4 PHASE MATCH

5.4.3 *Sellmeier equations*

The largest second order non-linearity is, as mentioned in Section 5.4.1, achieved by the interaction of field all polarized along the extraordinary axis of the crystal.
[Missing section reference.]

5.5 PULSE PROPAGATION

5.5.1 *Retarded time frame*

...and we assume that all field are polarized along the x-direction according to laboratory coordinates as...
[x-axis instead of y-axis.]

5.6 QUANTUM FLUCTUATION

Second harmonic generation depends only on the presence of the pump frequency and the process of generating the double frequency initializes even without the presence of the second harmonic wave. [Removed misplaced word *double*.]

...we estimate that an average pump power of 175 mW for a 7 ns pulse at a repetition rate of 200 µs gives a pump peak power of approximate 10 kW. This pump creates a signal pulse of peak power 180 mW. Inserting this into Equation 111 estimates the quantum fluctuations to 1.1 mW.
[200 µs instead of 20 µs. 10 kW instead of 1.1 mW.]

5.6.1 *Estimating the quantum noise level*

where g is the gain parameter and $a_{pump}(z)$ it the square root of the pump photon flux as defined in...
[Added *square root of the*.]

7.0 PLANE WAVES

Axis on Figure 16a is wrong. Should be the same as the one on Figure 16b.

8.1 SLIGHTLY CONFINED MODES

8.1.1 *Strong coupling*

$$P(n) = \left| \sum_{j=1\cdots n} a_j u_{j,0} \right|^2 \tag{118}$$

[Square of the numerical value of the sum. a_j instead of U_j.]

9.3 MEASUREMENTS

9.3.1 *Estimation of quantum noise level*

Using now that a pump power of 175 mW creates a non depleted pulse of power ≈ 8 mW and inserting this into Equation 111 yields

that $I_{signal}(0) = 100\,\text{kW}/\,\text{m}^2$.
[$I_{signal}(0) = 100\,\text{kW}/\,\text{m}^2$ instead of $I_{signal}(0) = 10\,\text{mW}/\,\text{m}^2$.]

If however a narrow seed of $\approx 100\,\text{kW}/\,\text{m}^2$ is applied then the simulation should approximate the configuration.
[$I_{signal}(0) = 100\,\text{kW}/\,\text{m}^2$ instead of $I_{signal}(0) = 10\,\text{mW}/\,\text{m}^2$.]

BIBLIOGRAPHY

[16] Manual documents version 3.3.3 of FFTW, Matteo Frigo and Steven G. Johnson, 2012
[Wrong title.]

Technical University of Denmark

Anders C. Bilfeldt: *Numerical modeling of optical parametric frequency conversion*, for temporally confined pulses and spatially confined modes, © August 2014

This thesis and all related material is avaliable for download at
http://www.anders.bilfeldt.dk/thesis/
alternatively use the Q-code above